Soil Biology and Biochemistry 163 (2021) 108455

Contents lists available at ScienceDirect

Soil Biology and Biochemistry

journal homepage: www.elsevier.com/locate/soilbio

Relating the spatial distribution of a tall-grass to fertility islands in a temperate mountain grassland

Leticia San Emeterio [a,*], María Durán [a], Leire Múgica [a], Juan J. Jiménez [b], Rosa Maria Canals [a]

[a] Institute on Innovation and Sustainable Development in Food Chain (IS-FOOD), Department of Agricultural Engineering, Biotechnology and Food, Public University of Navarre (UPNA), Arrosadia Campus, 31006, Pamplona, Spain
[b] ARAID, Pyrenean Institute of Ecology (IPE), Consejo Superior de Investigaciones Científicas (CSIC), Avda. Ntra. Sra. de la Victoria, 16, E-22700, Jaca, Huesca, Spain

ARTICLE INFO

Keywords:
Native invader
Fertility island
Geostatistics
Soil function
Brachypodium rupestre

ABSTRACT

Plant-soil feedback mechanisms influence the abundance and rarity of plant species and can favour invasive processes, including those of native species. To explore these mechanisms, we analysed correlations between spatial distributions of plant biomass and soil properties in two neighbouring grasslands at different phases of expansion of the native Eurasian tall-grass *Brachypodium rupestre* (Host) Roem & Schult (*B. rupestre* cover: >75 and 25–50%). For this, we applied spatially explicit sampling, geostatistical analysis and structural equation models (SEM) to probe causal relationships among measured variables involved in nutrient accumulation. We hypothesized that if litter accumulates as a result of reduced grazing, 'fertility islands' (spots of high SOM and nutrient contents) will form under *B. rupestre* clumps because the increase in resource inputs from litter will trigger SOM build-up and promote microbial growth. Our results show that 'fertility islands' of P and amino acids occurred under the patchy clumps of *B. rupestre* in the less invaded grassland. In addition, the SEMs indicated that nutrient accumulation was partially due to mineralization of the SOM and modulated by the soil microbial biomass. However, there was no correlation between spatial patterns of *B. rupestre* biomass, SOM and microbial biomass. Moreover, the SEMs explained small amounts of variance in them (SOM $r^2 = 0.22$ and microbial biomass $r^2 = 0.08$), suggesting that factors other than *B. rupestre* biomass were responsible for the high fertility below the patches. Our spatially explicit approach demonstrated that litter inputs in dense temperate grassland communities can generate 'fertility islands' that may favour the stability and expansion of a tall-grass invader and suggest that herbivory may enhance or inhibit this phenomenon.

1. Introduction

Plant-soil feedback mechanisms can contribute to the invasive behaviour of some perennial tall grasses that are extensively spreading into ecosystems throughout Europe and North America (Vinton and Goergen, 2006). Changes in disturbance regimes and human actions (relaxation of domestic grazing, recurrent burnings and fertilization) may trigger this invasive behaviour (Canals et al., 2017; Catorci et al., 2011; Holub et al., 2012). *Brachypodium rupestre* (Host) Roem & Schult is a tall-grass native to Eurasia that can outcompete and displace co-dominant species, creating grasslands with low diversity and forage quality, associated with disruption of traditional management regimes (Fig. 1). Understanding the mechanisms that favour expansion of this tall-grass and contribute to stabilisation of this low-diversity grassland community would help efforts to identify management practices that can prevent its expansion.

Plant-soil feedback processes influence species' abundance, either positively or negatively, thereby promoting increases and decreases in their abundance, respectively (van der Putten et al., 2013). They play major roles in invasive processes (Klironomos, 2002; Suding et al., 2013) and stabilisation of alternate states (Rietkerk and van de Koppel, 1997; Suding et al., 2004). One well-known feedback process involves plants inducing accumulation of soil organic matter (SOM), which reciprocally promotes plant growth. One well-known feedback process involves plants inducing accumulation of soil organic matter (SOM), which reciprocally promotes plant growth. A well-studied example is the formation of 'fertility islands' under shrubs and grass tussocks in arid and semi-arid areas (Gutiérrez et al., 1993; Schlesinger and Pilmanis, 1998).

* Corresponding author. Research Institute on Innovation & Sustainable Development in Food Chain (ISFOOD), Universidad Pública de Navarra, Pamplona, 31006, Spain.
E-mail address: leticia.sanemeterio@unavarra.es (L. San Emeterio).

https://doi.org/10.1016/j.soilbio.2021.108455
Received 23 April 2021; Received in revised form 29 September 2021; Accepted 6 October 2021
Available online 7 October 2021

In this process, higher litter inputs under the plant canopies than in areas with bare soil may enhance soil microbial biomass and activity, leading to accumulation of SOM and, hence, an increase in nutrient availability. Patches of *B. rupestre* developing within high-diversity grasslands are grazed much less intensively than the surrounding vegetation, so its biomass accumulates, producing a thick layer of dead matter. Hurst and John (1999) detected more nitrate in soils under patches of *B. rupestre* than in adjacent soils suggesting that *B. rupestre* may create fertility islands, similar to those created under shrubs in arid and semi-arid ecosystems. The fertility island hypothesis has been tested by comparing vegetated and bare soil microhabitats in arid and semi-arid plant communities, but not in humid temperate grasslands with continuous vegetation cover.

Our objectives in the study presented here were to determine if nutrients and soil organic matter (SOM) accumulate under *B. rupestre* patches, creating fertility islands, and if these islands disappear with the consolidation of *B. rupestre* monodominance promoted by the recurrence of burnings. We hypothesized that if litter accumulates under *B. rupestre* clumps (Fig. 1b), fertility islands will be established (spots with high SOM and nutrient contents) due to the increase in resource inputs. In contrast, in frequently burned *B. rupestre* grasslands (Fig. 1c), fire will prevent litter accumulation, so the fertility island effect will disappear. To test whether the fertility-island effect occurs in the focal humid temperate grassland with continuous vegetation cover, we applied spatially explicit sampling, geostatistical analysis and piecewise structural equation modelling to study spatial patterns of *B. rupestre* biomass and soil variables. We examined the patterns in both a *B. rupestre* monodominant grassland (*B. rupestre* cover >75%, Fig. 1c) and a grassland that had not been completely invaded, where *B. rupestre* patches coexisted with high-diversity patches (*B. rupestre* cover 25–50%, Fig. 1b). We specifically tested two contrasting models. According to one, *B. rupestre* biomass and litter influence soil microbial biomass and SOM directly and soil nutrient availability indirectly (Figure S1, SM1). According to the other model, soil microbial biomass and SOM directly influence nutrient availability for the growth of *B. rupestre* after burning (Figure S2, SM1).

2. Material and methods

2.1. Study site

Empirical data were acquired at a site on the Spanish-French border between the Aezkoa (Spain) and Cize (France) valleys in the Western Pyrenees (43°2′ N, 1°10′ W; Fig. 2). The mean annual temperature and precipitation here are 9.3 °C and 1890 mm, respectively, according to data collected during 1989–2019 at the nearest climatic station, Irabia, located ca. 5 km from the sampling plots at 822 m asl (Gobierno de Navarra, n.d.). Soils at the site, which developed from sandstones and calcareous clays, are acidic (pH 4.3–5.3) with high organic matter content (5.8–14.5% SOM content) and loamy or clay-loamy textures (See Table 1 for a classification of the soils). The vegetation is a mosaic of beech forests, shrubland communities dominated by *Ulex gallii* Planch. and *Erica vagans* L., and grassland communities dominated by perennial grasses such as *Festuca rubra* gr., *Agrostis capillaris* L., *B. rupestre*, *Danthonia decumbens* (L.) DC. and *Avenula sulcata* (J. Gay ex Boiss.) Dumort., forbs such as *Galium saxatile* L., *Potentilla erecta* (L.) Räeusch and *Hipochaeris radicata* L., and legumes such as *Trifolium repens* L.

The area is a communal pastureland grazed by French and Spanish livestock. Free-ranging sheep, cows and horses use these grasslands during the mild season (from May to October). Domestic herbivores intensively grazed the area for centuries, but due to socio-economic changes during the second half of the 20th century and depopulation of the rural areas livestock numbers have declined by ca. 50% in the last two decades, which has facilitated the expansion of *B. rupestre* in many areas. Every year *B. rupestre* builds up a ca. 5 tonnes/ha layer of dead matter, which is frequently eliminated by winter surface burnings. Consequently, the traditional pastoral fire regime to prevent shrub encroachment (every 6–7 years on uneven clumps of ungrazed vegetation) has been replaced by a new regime with more frequent fires (every 2–4 winters) in the less intensively grazed areas (Canals et al., 2019). Usually, in these low-severity burnings of grasslands the soil is heated to 30–60 °C at 5 cm depth and ca. 200 °C at the surface (Múgica et al., 2018; Úbeda et al., 2005).

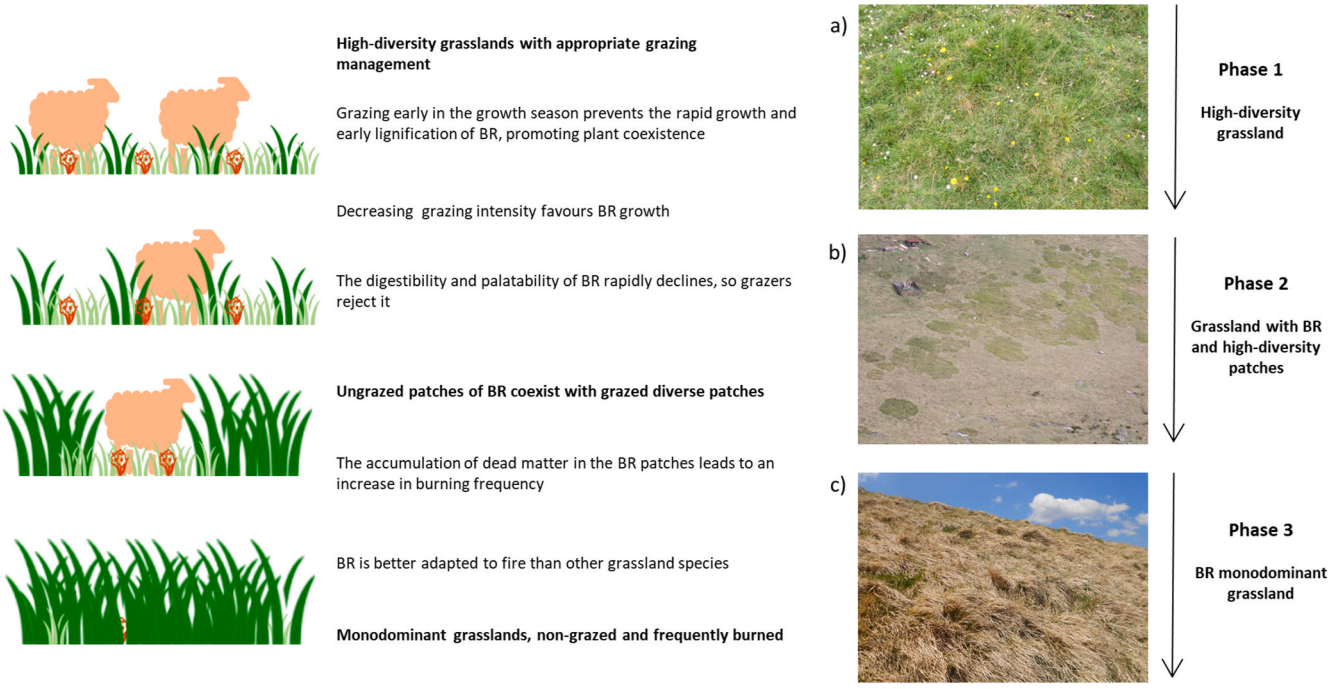

Fig. 1. Observed phases of *B. rupestre* expansion in the Western Pyrenees.

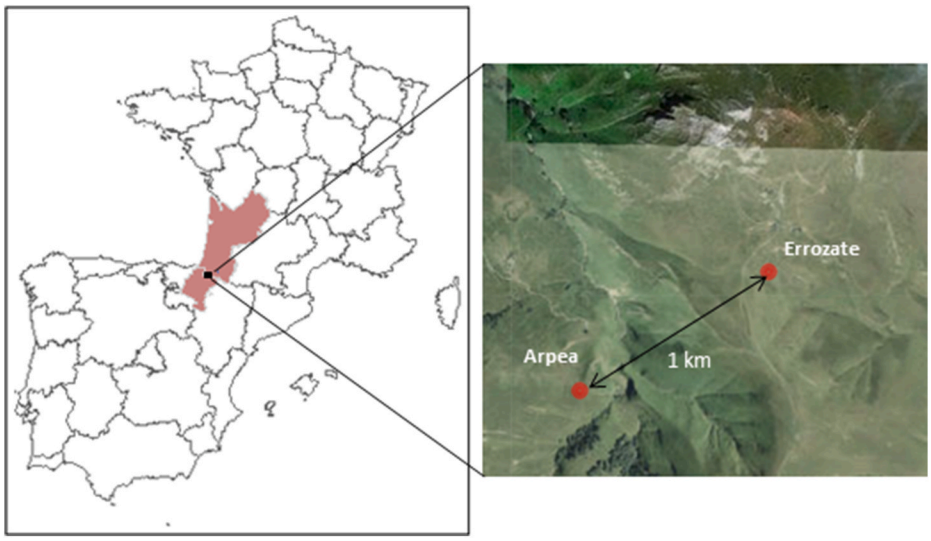

Fig. 2. Location of the study area showing Navarra in Spain and Aquitaine in France (shaded), and the sampling sites in Arpea (monodominant grassland) and Errozate (patchy grassland).

Table 1
General description of the study sites.

Site	Grassland type	Altitude (m asl)	Slope (°)	Aspect	Soil types
Errozate	*B. rupestre*-patched	1091	33	NW	Lithic Udorthents
Arpea	*B. rupestre*- monodominant	943	26	NE	Typic Dystrudepts

2.2. Sampling design

A 12 × 12 m plot was established in a *B. rupestre* patchy grassland in Errozate (1091 m asl) and one in a monodominant grassland 1 km away in Arpea (943 m asl) (Fig. 2), where the *B. rupestre* cover was <50% and >80%, respectively. Table 1 summarizes selected characteristics of both locations. We systematically sampled soil and vegetation at the nodes of a grid of 8 × 8 sampling points with 1.5 m spacing. The sampling was designed to capture the spatial structure of *B. rupestre* cover distribution in the patchy grassland, where *B. rupestre* patches have diameters of ca. 3 m, so the 1.5 m sampling distance ensured the acquisition of replicate samples of patches within the grid. We sampled the patchy grassland in late May 2017 and the monodominant grassland in early June 2017. The patchy grassland had not been burned for at least 8 years and the monodominant grassland was burned at the end of the previous winter (as part of a biennial cycle). At each of the 64 sampling points in each plot, we took two soil cores: one of 6 cm diameter and 10 cm depth for analysis of soil parameters and the other of 4.5 cm diameter and 10 cm depth for belowground plant biomass estimations. Soil samples were kept at 4 °C until analysis. We also established a subplot of 15 × 15 cm per sampling point, in which we recorded the plant species present and harvested the vegetation at ground level. The aboveground biomass was separated into dead and green fractions, and the green biomass was further separated into species. The plant material was oven-dried at 65 °C for 72 h and its dry weight was recorded. The belowground biomass in the subplot was also collected, cleaned with water, separated into two categories (rhizomes solely of *B. rupestre* and roots of both *B. rupestre* and other plants), dried and weighed. This provided estimates of total root biomass in both grasslands and *B. rupestre* root biomass in the monodominant grassland, where *B. rupestre* dominance was sufficiently high to ignore contributions of other species to the root biomass. We could not obtain estimates of *B. rupestre* root biomass in the patchy grassland since we could not separate roots into species or distinguish *B. rupestre* roots from other species. We calculated *B. rupestre* dominance as the percentage of *B. rupestre* biomass in the total aboveground biomass.

2.3. Soil analysis

We measured soil physico-chemical parameters, soil nutrients, soil enzyme activities and soil microbial biomass. The soil parameters were analysed as described by Canals et al. (2019). Briefly, the main physical and chemical parameters were determined by standard methods in a certified laboratory (Nasertic, Pamplona, Spain): SOM by oxidation with chromate in the presence of sulfuric acid, total N by the Dumas method, available P by the Olsen method and exchangeable Al by titration. The soil water content (SWC) was measured gravimetrically. Ammonium and nitrate pools were extracted in 2 M KCl, then quantified using an AA3 segmented flow analyser (Braun + Luebbe, Norderstedt, Germany). Microbial biomass C and N (MBC and MBN, respectively) contents were determined by chloroform fumigation-direct extraction (Davidson et al., 1989), assuming a fumigation efficiency of 0.54 (K_N and K_C) (Joergensen et al., 2011). Dissolved organic carbon (DOC) and dissolved organic nitrogen (DON) contents were measured and calculated as described by San Emeterio et al. (2014). Soil enzyme activities were determined in homogenised and freshly-sieved (2 mm) soil samples. β-glucosidase and acid phosphatase activities were measured using a 96-well microplate approach (German et al., 2011) as described by San Emeterio et al. (2016). Urease activity was measured following the method published by Kandeler and Gerber (1988) and modified byRodriguez-Loinaz et al. (2008). Microbial biomass and enzyme activities were determined within 2 weeks after soil sampling. Total amino acid contents were determined following the spectrofluorometric method presented by Jones et al. (2002) and modified by Darrouzet-Nardi et al. (2013).

2.4. Statistical analyses

We used geostatistical techniques implemented in R (R Core Team, 2018) to evaluate the above- and below-ground spatial patterns of biomass and soil properties in our grasslands, regarded as representing

two phases of *B. rupestre* expansion.

2.4.1. Spatial autocorrelation

We used the coefficient of variation (CV) as a measure of global variation in the vegetation and soil parameters, and correlograms and semi-variogram modelling to assess spatial autocorrelation (local variation) (Das Gupta et al., 2015).

We applied correlogram analysis with Moran's I index to assess the significance of the spatial patterns of plant and soil variables (Legendre and Fortin, 1989), regarding a correlogram as statistically significant if at least one coefficient was significant at $p < 0.05$ after Holm correction (Borcard et al., 2018).

Semi-variograms were adjusted to the most commonly used models (nugget, spherical, exponential and wave). We assumed that there was no spatial dependence for distances larger than the range. (See SM2 for details of lag distances and fitting of the semi-variograms). Greater CV values and shorter spatial autocorrelation ranges indicate greater spatial heterogeneity. We used the nugget to total variance ratio to determine spatial dependency, and classified it as weak (<0.25), moderate (0.25–0.75, or strong (>0.75) (Cambardella and Elliott, 1994). We estimated values of the variables at non-sampled points by 'ordinary kriging' interpolation using the four semi-variograms (Cressie, 1993). We subjected the models to leave-one-out cross-validation and used the root mean square error (RMSE) as a measure of precision, mean error (ME) as a measure of bias and mean squared deviation ratio (MSDR) of the residuals to the prediction error, which is close to one for a correctly specified model. We selected the model with the lowest RMSE and in case of a tie the model with the MSDR closest to 1. Map contours were generated with the best model for each variable. Semivariogram plots and the models' cross-validation statistics are presented in the supplementary material (SM3). We used the ncf R package to construct the correlograms (Bjornstad, 2018) and the gstat R package (Gräler et al., 2016) for calculating and adjusting the semi-variograms, the kriging, and contour maps.

2.4.2. Spatial associations

We used cross-correlograms to study the spatial associations between *B. rupestre* biomass and soil variables (Jiménez et al., 2011, 2014). A cross-correlogram shows the correlation between two variables separated by some lag and represents the correlation for all the distances of interest. At zero distance, the correlation is equal to the Pearson correlation coefficient. To test the hypothesis that 'fertility islands' were present in the sampled areas we compared cross-correlograms and map contours (spatial distribution of patches) of *B. rupestre* shoot biomass and soil variables. We considered that fertility islands were present if the size (range of the semivariograms) and spatial distribution of patches were similar and the cross-correlogram was significant at short, but not longer, distances.

2.4.3. Piecewise structural equation models

We used piecewise SEMs to construct a probabilistic model representing the relationships between response and predictor variables using a network of pathways, each representing a hypothesized causal relationship based on prior studies and scientific knowledge. A good fit does not prove a causal assumption, but indicates that it is plausible (Bollen and Pearl, 2013). In this sense, rather than deriving causal relationships from the model, we were interested in testing whether our data supported the conceptual model (see SM1). We used piecewiseSEM and nlme packages (Lefcheck, 2016; Pinheiro et al., 2018) to fit a battery of general least square models with spatially autocorrelated errors that were combined into a network of pathways. We tested effects of *B. rupestre* litter inputs on microbial biomass, SOM and ultimately nutrient availability in the *B. rupestre*-patched grassland (Figure S1 in SM1). In the *B. rupestre*-dominated grassland, the fire in the previous year had eliminated most of the litter and we lack data on the distribution of ash after the fire. Thus, we could not model nutrient inputs in the ecosystem and did not expect a good fit for the model of relationships in this grassland. Instead, we decided to test effects of microbial biomass on SOM, nutrient availability and ultimately the *B. rupestre* biomass production after fire (Figure S2 in SM1). More details on the models and a detailed justification for the pathways can be found in the supplementary material (SM1).

3. Results

3.1. Descriptive statistics

The soil in the monodominant grassland had slightly higher pH but lower nutrient contents and microbial biomass than the soil in the patchy grassland. Activities of soil enzymes involved in C and P cycles were higher in the monodominant than in the patchy grassland soil, but the activity of urease (involved in N cycling) was higher in the patchy grassland soil (Table 2). The variability of most measured soil parameters was similar in the two grasslands. However, CVs for nitrate content, DON content and C:N ratio were substantially higher in the monodominant grassland soil than in the patchy grassland soil.

B. rupestre patches covered approximately 30% of the plot in the patchy grassland and was locally dominant (cover >60%) at 12% of the sampling points. In the monodominant grassland, *B. rupestre* cover exceeded 95% in the whole plot and 80% at 94% of the sampling points. The total green aboveground biomass was twice as high in the patchy grassland as in the monodominant grassland, but the total belowground biomass in the plots was very similar (Table 2). In the patchy grassland, the dead biomass was almost twice as high as the total green aboveground biomass, whereas in the monodominant grassland the dead biomass had been consumed by the previous burning except at a few points (Table 2). We found greater variability in all plant variables (higher CVs) in the patchy than in the monodominant grassland, except for dead biomass (Table 2).

3.2. Spatial patterns and spatial autocorrelation

3.2.1. Plant biomass variables

Biomass of *B. rupestre* had strongly heterogeneous spatial structure in the patchy grassland and no significant spatial structure in the monodominant grassland according to the correlograms and semi-variograms. Moran's I correlograms indicated significant spatial autocorrelation of *B. rupestre* biomass variables, including positive spatial autocorrelation in green biomass of the species at distances less than 4 m, in the patchy grassland (Fig. 3). These results are consistent with the semi-variograms. Spherical models provided the best fits to semi-variograms for *B. rupestre* biomass variables in the patchy grassland, except for the rhizome biomass (for which a wave model was best). Their ranges varied from ca. 2 m for rhizomes and ca. 4 m for shoot biomass (Table 3 and Figure S3 in SM3). The distribution of the total aboveground biomass in the patchy grassland had much weaker spatial dependence than the *B. rupestre* biomass, reflecting the high production in *B. rupestre* patches and much lower production in the diverse patches (Table 3). We detected no significant spatial structure in the total belowground biomass, although we found clumps of *B. rupestre* rhizomes.

In contrast, the correlograms indicated that the only spatially autocorrelated biomass variables at short distances (<2.5 m) in the monodominant grassland were *B. rupestre* root and total belowground biomass (Fig. 3). The semi-variogram for the *B. rupestre* root biomass was adjusted to an exponential model with a range (166 m) well above the maximum sampling distance (Table 3). For the rest of the biomass variables the correlograms were not significant (Fig. 3) and no spatial structure was found at the scale of this study (Table 3, Figure S4 in SM3).

3.2.2. Soil variables

In the patchy grassland, we detected strong spatial structure in the physicochemical variables but weak, or no, spatial structure in

Table 2
Descriptive parameters of plant biomass and soil variables of the *B. rupestre*-patched and *B. rupestre*-monodominant grasslands.

Variable[a]	Site	Mean	SD	Median	Skewness	Kurtosis	CV
Plant biomass (kg ha^{-1})							
B. rupestre shoots	Patchy	655	781	258	1.24	0.51	119
	Monodominant	853	484	793	0.60	0.23	56.7
B. rupestre rhizomes	Patchy	416	739	0.00	2.07	3.98	177
	Monodominant	1900	1300	1700	1.15	1.78	71.2
B. rupestre roots	Patchy	Data not available					
	Monodominant	5020	2200	4840	0.24	−0.28	43.9
Total aboveground	Patchy	1890	1380	1500	1.80	3.59	72.9
	Monodominant	884	481	835	0.60	0.10	54.5
Total belowground	Patchy	7040	3660	6030	0.84	0.05	51.0
	Monodominant	7270	2690	7120	0.44	0.05	37.1
Litter	Patchy	1180	1520	457	1.98	3.70	129
	Monodominant	62.7	221	4.89	4.89	23.8	352
BR dominance (%)	Patchy	27.6	23.9	18.9	0.84	−0.34	86.4
	Monodominant	94.4	16.1	100	−3.97	17.6	17.0
Soil physicochemical parameters							
SWC (kg kg^{-1})	Patchy	0.37	0.04	0.37	−0.32	−0.52	10.4
	Monodominant	0.35	0.04	0.35	−0.29	−0.18	10.8
pH	Patchy	4.62	0.10	4.63	−0.32	0.22	2.19
	Monodominant	5.01	0.14	5.00	0.40	0.60	2.70
C:N	Patchy	11.2	0.68	11.2	0.04	−0.67	6.05
	Monodominant	10.2	1.04	10.1	1.05	1.88	10.1
DOC (mg C kg^{-1})	Patchy	108	24.7	104	2.46	10.2	22.8
	Monodominant	44.3	11.9	43.4	−0.12	0.36	26.9
SOM (g kg^{-1})	Patchy	109	156	110	0.12	−0.87	14.3
	Monodominant	7.71	1.10	7.56	1.13	0.95	14.27
Al (cmol (+) kg^{-1})	Patchy	6.22	0.68	6.27	−0.31	−0.47	11.0
	Monodominant	Data not available					
Soil nutrients							
P (mg P_2O_5 kg^{-1})	Patchy	9.00	4.32	8.84	0.26	−1.03	48.0
	Monodominant	5.07	2.65	4.60	1.28	1.53	52.3
Nitrate (mg N kg^{-1})	Patchy	0.39	0.13	0.38	1.01	2.05	33.6
	Monodominant	0.51	0.16	0.47	4.88	29.3	31.9
Ammonium (mg N kg^{-1})	Patchy	6.28	1.78	5.90	2.62	10.4	28.4
	Monodominant	4.60	1.59	4.01	1.70	2.28	34.5
Total Aa (μmol kg^{-1})	Patchy	622	104	605	0.16	−0.56	16.7
	Monodominant	464	81.8	450	−0.01	−0.03	17.6
DON (mg N kg^{-1})	Patchy	21.9	4.77	21.1	2.33	6.98	21.7
	Monodominant	10.6	3.93	10.4	1.14	3.51	37.2
Total N (g kg^{-1})	Patchy	5.7	0.8	5.6	0.26	−0.33	13.7
	Monodominant	4.4	0.5	4.3	0.98	0.95	12.1
Soil enzyme activities							
Urease (mg N kg^{-1} h^{-1})	Patchy	49.1	10.5	48.4	0.64	0.77	21.4
	Monodominant	27.5	7.21	26.3	0.45	−0.31	26.2
Phosphatase (nmol PN k^{-1} h^{-1})	Patchy	203	40.8	191	0.95	0.40	20.1
	Monodominant	242	37.2	247	0.06	−0.98	15.3
Glucosidase (nmol PN g^{-1} h^{-1})	Patchy	82.8	11.9	81.5	−0.30	−0.08	14.4
	Monodominant	95.8	11.1	93.8	0.02	−0.44	11.6
Soil microbial biomass							
MBC (mg C kg^{-1})	Patchy	1110	322	1090	0.55	0.56	28.8
	Monodominant	586	106	570	1.37	2.08	18.1
MBN (mg N kg^{-1})	Patchy	870	141	869	0.30	−0.02	16.2
	Monodominant	545	126	544	−0.74	1.53	23.2

[a]SWC, soil water content; DOC, dissolved organic carbon; SOM, soil organic matter; Aa, amino acids; DON, dissolved organic nitrogen; PN, p-nitrophenol; MBC, microbial biomass carbon; MBN, microbial biomass nitrogen.

distributions of soil nutrients (Table 3, Fig. 3). All the correlograms for soil physicochemical variables except DOC were significant and indicated positive autocorrelations at the shortest distance classes (Fig. 3). Accordingly, semi-variograms were adjusted to spheric models for SWC, pH and C/N ratio, and to exponential models for SOM and aluminium. The ranges varied between 2.2 and 5.7 m for SWC and SOM, respectively. No spatial structure in the distribution of DOC was detected at the scale of this study (Table 3, Figure S3 in SM3). In contrast, no correlograms for soil nutrients, soil enzyme activities or soil microbial biomasses in the patchy grassland were significant at short distances except for amino acids ($p < 0.10$) (Fig. 3). Despite the lack of significance of the correlograms, we obtained semi-variograms with adequate fits for some of these soil variables. P, ammonium, phosphatase and MBN were adjusted to wave models, and amino acids and MBC to spherical models, with ranges varying between 1.6 and 7.6 m for phosphatase and MBC, respectively (Table 3, Figure S3 in SM3).

In the monodominant grassland, no spatial structure was detected in the soil physicochemical variables, but we found spatial dependence for some soil nutrients, soil enzyme activities and soil microbial biomass (Table 3, Fig. 3). We obtained no significant correlograms for soil physicochemical variables (Fig. 3), and accordingly we found no spatial structure at the scale of this study for these soil variables (Table 3, Figure S4 in SM3). For soil nutrients we obtained significant correlograms with positive autocorrelations at the shortest distance classes for P and amino acids (Fig. 3). Accordingly, we adjusted semi-variograms to a spherical model for P and amino acids. We were also able to adjust the semi-variograms of ammonium and DON to spherical and exponential models, respectively. Ranges of these semi-variograms varied between 1.1 and 4.7 m for DON and ammonium, respectively (Table 3, Figure S4 in SM3). For the other soil nutrients we obtained non-significant

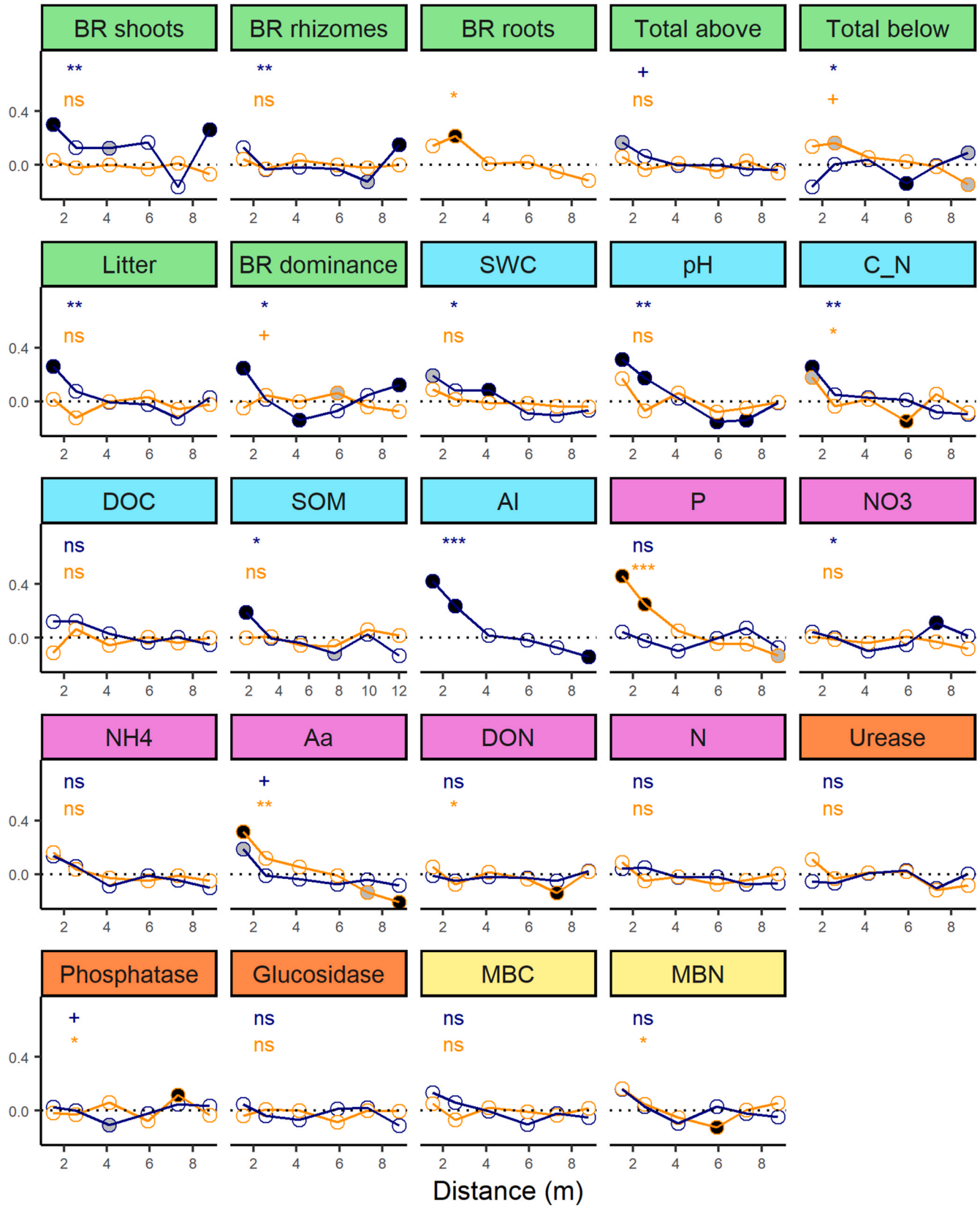

Fig. 3. Correlograms of plant variables (light green), soil physicochemical variables (light blue), soil nutrients (pink), soil enzyme activities (orange) and microbial biomass (yellow) in the *B. rupestre*-patchy grassland (navy blue lines) and *B. rupestre*-monodominant grassland (orange lines). Black, grey and open circles indicate $p < 0.05$, $p < 0.10$, and no significant correlation at the corresponding distance classes. Overall significance: ns, $p > 0.10$; +, $p < 0.10$; *, $p < 0.05$, **, $p < 0.01$; ***, $p < 0.001$. BR, *Brachypodium rupestre*; SWC, soil water content; DOC, dissolved organic carbon; SOM, soil organic matter; Aa, amino acids; DON, dissolved organic nitrogen; MBC, microbial biomass carbon; MBN, microbial biomass nitrogen. (For interpretation of the references to colour in this figure legend, the reader is referred to the Web version of this article.)

Table 3
Parameters of the best fitted semi-variograms for *B. rupestre* biomass and soil variables of the patchy and monodominant grasslands.

Variable[a]	site	Model[b]	Nugget	Sill	Range	Spatial dependence	Dependence class	r2
Plant biomass								
BR shoots	Patchy	Sph	0.072	0.411	3.76	0.82	Strong	0.999
	Monodominant	Nug	0.149					0.906
BR rhizomes	Patchy	Wave	0.005	0.018	2.23	0.38	Moderate	0.996
	Monodominant	Nug	0.022					0.939
BR roots	Patchy		Data not available					
	Monodominant	Exp	0.085	1.08	166	0.92	Strong	0.999
Total aboveground	Patchy	Sph	0.324	0.494	4.31	0.34	Moderate	0.996
	Monodominant	Nug	0.136					0.949
Total belowground	Patchy	Nug	0.294					0.975
	Monodominant	Nug	0.150					0.962
Litter	Patchy	Sph	0.162	0.50	3.75	0.68	Moderate	0.999
	Monodominant	Nug	0.119					0.958
BR dominance	Patchy	Exp	0.00	7.50	1.25	1	Strong	0.999
	Monodominant	Nug	1.49					0.951
Soil physicochemical parameters								
SWC	Patchy	Sph	0.000	0.000	2.21	1	Strong	0.993
	Monodominant	Nug	0.001					0.971
pH	Patchy	Sph	0.004	0.01	4.5	0.42	Moderate	0.999
	Monodominant	Nug	0.017					0.976
C_N	Patchy	Sph	0.000	0.42	2.64	1	Strong	0.997
	Monodominant	Wav	0.001	0.01	1.7	0.91	Strong	0.991
DOC	Patchy	Nug	493					0.965
	Monodominant	Nug	143					0.971
SOM	Patchy	Exp	1.580	2.96	5.57	0.47	Moderate	0.997
	Monodominant	Wave	0.564	1.22	1.66	0.54	Moderate	0.989
Al	Patchy	Exp	0.035	0.513	2.31	0.93	Strong	0.999
	Monodominant	Data not available						
Soil nutrients								
P	Patchy	Wave	0.266	0.296	3.18	0.1	Weak	0.981
	Monodominant	Sph	0.029	0.289	2.94	0.9	Strong	0.999
Nitrate	Patchy	Nug	0.059	0.066	3.13	0.1	Weak	0.974
	Monodominant	Nug	0.064					0.922
Ammonium	Patchy	Wav	0.047	0.058	3.76	0.18	Weak	0.996
	Monodominant	Sph	0.053	0.089	4.72	0.40	Moderate	0.999
Total Aa	Patchy	Sph	0.002	0.011	2.96	0.78	Strong	0.999
	Monodominant	Sph	0.000	0.007	2.88	1	Strong	0.999
DON	Patchy	Nug	24.900					0.943
	Monodominant	Exp	5.300	17.1	1.1	0.69	Moderate	0.981
Total N	Patchy	Nug	0.006					0.975
	Monodominant	Nug	0.014					0.973
Soil enzyme activities								
Urease	Patchy	Nug	108					0.925
	Monodominant	Nug	51.3					0.977
Phosphatase	Patchy	Wave	1140	1360	1.6	0.16	Weak	0.932
	Monodominant	Wave	1170	1370	1.66	0.14	Weak	0.904
Glucosidase	Patchy	Nug	144					0.972
	Monodominant	Nug	123					0.933
Microbial biomass								
MBC	Patchy	Sph	0.064	0.094	7.56	0.32	Moderate	0.998
	Monodominant	Wave	0.011	0.028	1.55	0.61	Moderate	0.986
MBN	Patchy	Wave	0.017	0.024	2.67	0.29	Weak	0.996
	Monodominant	Wav	0.071	0.102	3.71	0.31	Moderate	0.999

[a]SWC, soil water content; DOC, dissolved organic carbon; SOM, soil organic matter; Aa, amino acids; DON, dissolved organic nitrogen; MBC, microbial biomass carbon; MBN, microbial biomass nitrogen.
[b]Nug, nugget; Sph, spherical; Exp, exponential.

correlograms (Fig. 3) and detected no significant spatial structure (Table 3, Figure S4 in SM3). For soil enzyme activities and soil microbial biomasses we obtained significant correlograms for phosphatase and MBN, but with no significant autocorrelation at the shortest distances. We adjusted the semi-variograms of phosphatase, MBN and MBC to a wave model, with ranges between 1.6 and 3.7 m for microbial biomass and phosphatase, respectively (Table 3, Figure S4 in SM3). We obtained no significant correlograms for the other enzyme activities (Fig. 3) and detected no spatial structure at the covered scale (Table 3, Figure S4 in SM3).

Spatial correlation ranges for soil variables in the monodominant grassland were similar to, or smaller, than those in the patchy grassland, except for ammonium (4.7 and 38 m in the monodominant and patchy grassland, respectively) and MBN (3.7 m and 2.6 m in the monodominant and patchy, grassland). Extrapolated ranges (above or below the maximum and minimum sampling distance, respectively) for variables such as *B. rupestre* root biomass and DON in the monodominant grassland, and *B. rupestre* cover in the patchy grassland, should be interpreted with caution.

3.3. Spatial associations between plant and soil variables in the patchy grassland

In the patchy grassland, we detected similar patterns in the spatial associations of *B. rupestre* shoot and rhizome biomass with some soil variables (Fig. 4). Positive correlations with *B. rupestre* shoot biomass at the shortest distances were found with C/N ratio, SOM and amino acids. An opposite pattern was found for pH, with a negative correlation in the

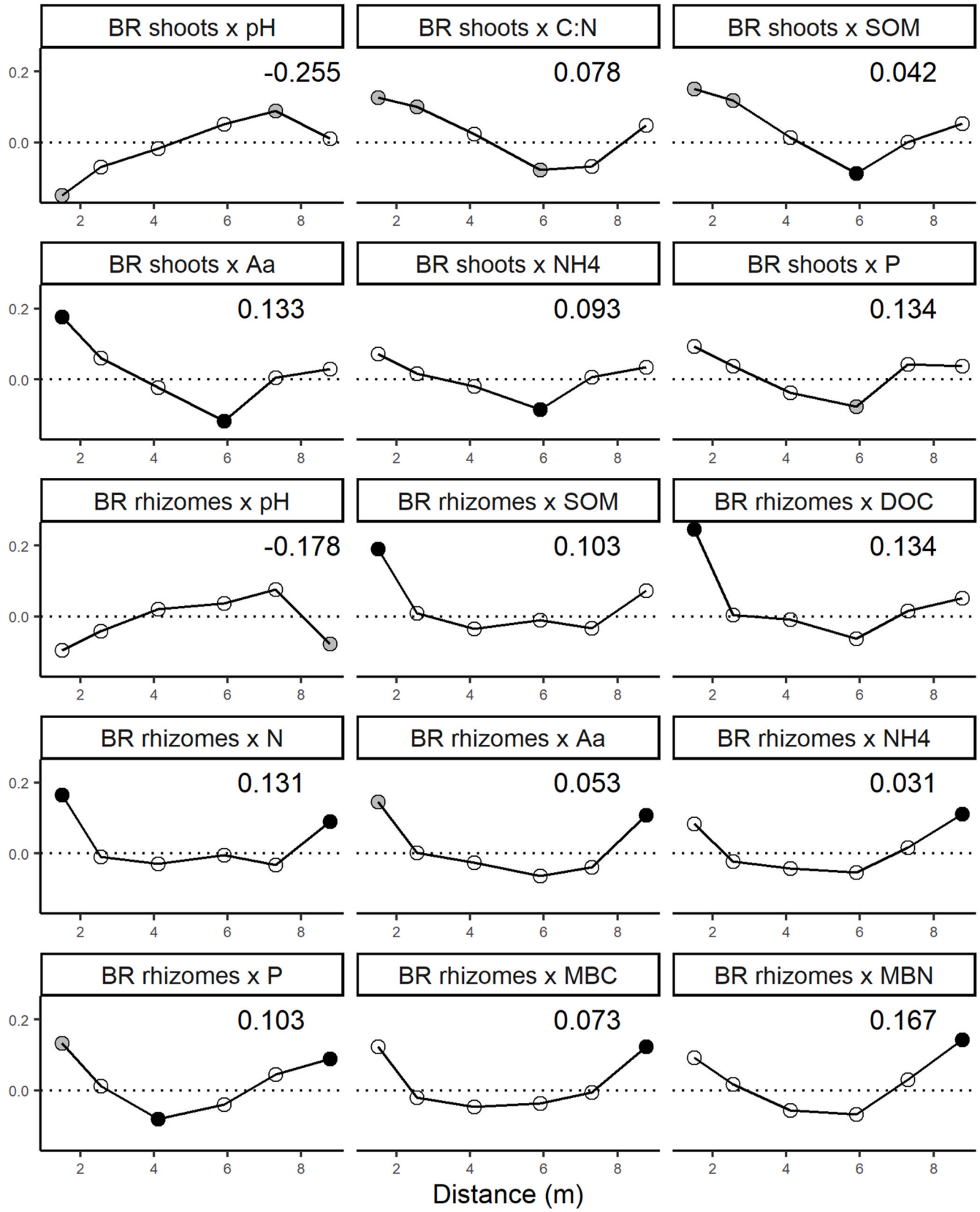

Fig. 4. Cross-correlograms of *B. rupestre* (BR) shoot and rhizome biomasses with soil variables in *B. rupestre* patchy grassland. Black, grey and open circles indicate $p < 0.05$, $p < 0.10$ and no significant correlation at the corresponding distance class, respectively. The correlation at zero distance is indicated below each sub-plot title. Aa, amino acids; SOM, soil organic matter; DOC, dissolved organic C; MBC, microbial biomass C; MBN, microbial biomass N.

shortest distance class (Fig. 4). For *B. rupestre* rhizomes, the spatial association pattern showed positive correlations at the shortest distance with SOM, DOC, N, amino acids, and P. All the cross-correlograms of the shoot and rhizome biomass with the soil variables are listed in the supplementary material (Tables S1 and S2 of SM4).

Patches of high *B. rupestre* shoot biomass coincided with patches of high P and Aa concentrations, but not patches of high ammonium concentration (Fig. 5). Patches of *B. rupestre* shoots also coincided with areas with high SOM and MBC, but the patch sizes of both soil variables were considerably larger than the patch size of the *B. rupestre* shoot biomass. Regarding pH, hot-spots of acidity approached the contour of *B. rupestre* shoot patches (Fig. 5). Contour maps for other plant and soil variables in the patchy grassland are shown in Figures S5 (SM5) and for biomass and soil variables in the monodominant grassland in Figure S6 (SM5).

3.4. Structural equation models

The proposed model for the relationships in the *B. rupestre*-patched grassland provided a good fit with the acquired data (Fisher's C = 34.54; df = 32; p = 0.347). In this grassland, *B. rupestre* biomass was clearly correlated positively with the availability of the nutrients amino acids, ammonium and P (Fig. 6a). Moreover: the abundance of litter was positively affected by production of *B. rupestre* biomass ($p < 0.001$), positively correlated with MBC ($p = 0.030$) and negatively correlated with pH (0.028). In addition, pH and SOM were significantly negatively correlated ($p = 0.002$), MBC and MBN were positively correlated ($p = 0.007$), MBC was positively correlated with Aa availability (0.039), while MBN was negatively correlated with both SOM ($p < 0.001$) and P availability ($p = 0.020$). SOM was positively correlated with amino acids, ammonium, and P availability ($p = 0.004$, $p = 0.037$ and $p < 0.001$, respectively), and amino acid contents were positively correlated with ammonium and nitrate contents ($p < 0.001$ and $p = 0.003$, respectively). Finally, variations in nutrient availability were better explained ($r^2 = 0.62$, 0.50, 0.36 and 0.15 for ammonium, P, amino acids and nitrate, respectively) and SOM ($r^2 = 0.22$) than variations in microbial biomasses ($r^2 = 0.08$ and 0.00 for MBC and MBN, respectively.

The proposed model for the *B. rupestre*-monodominant grassland also provided a good fit to the data (Fisher's C = 24.1; df = 20; p = 0.238). In this frequently burned grassland, the abundance of microbial biomass positively affected the incorporation of SOM into the soil, nutrient availability, and ultimately production of *B. rupestre* biomass after fire (Fig. 6b). In more detail, MBN and MBC were positively correlated ($p = 0.003$), while MBN was positively correlated with SOM ($p = 0.052$) and amino acid availability ($p = 0.006$). In addition, SOM was positively correlated with availability of both P ($p < 0.001$) and amino acids ($p = 0.048$), negatively correlated with ammonium availability ($p = 0.011$), and not significantly correlated with pH ($p = 0.335$). Moreover, amino acid availability was negatively correlated with nitrate availability nitrate ($p = 0.002$) and positively correlated with ammonium availability ($p < 0.001$), which was positively correlated with nitrate availability ($p < 0.001$). Finally, *B. rupestre* biomass was positively correlated with P and amino acid availability ($p = 0.001$ and $p < 0.001$, respectively), but negatively correlated with ammonium and nitrate availability ($p = 0.029$ and $p = 0.019$, respectively). The model explained between 25 and 37% of the variance in nutrient availability ($r^2 = 0.25$, 0.28, 0.30 and 0.37 for amino acids, P, ammonium and nitrate, respectively) and 38% of the variance in *B. rupestre* shoot biomass production.

4. Discussion

4.1. Fertility islands in the patchy BR grassland and potential plant-soil feedback pathways

Results of our measurements and spatially explicit modelling indicate that we can partially accept the tested hypothesis: some nutrients accumulated under *B. rupestre* clumps, but their accumulation can only

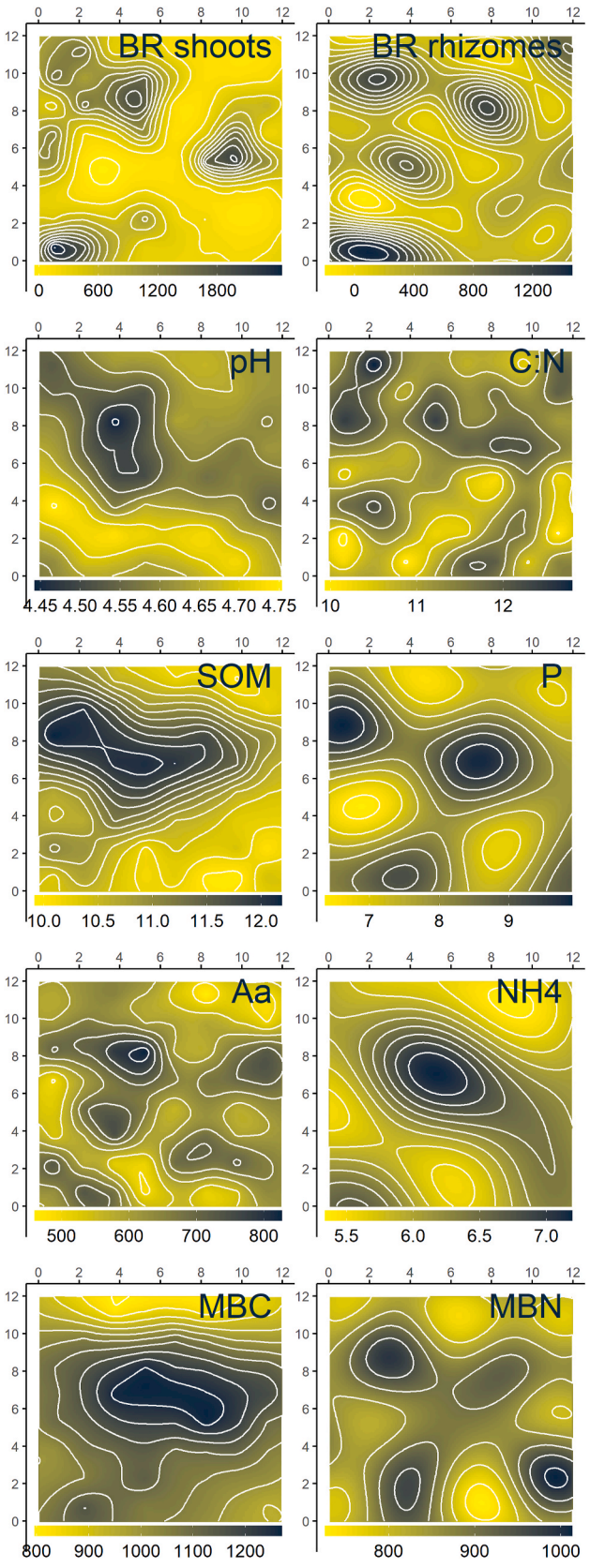

Fig. 5. Contour maps of B. rupestre (BR) biomass and soil variables in the patchy grassland. B. rupestre shoot and rhizome biomass (kg ha−1), Phosphorus (mg P2O5 kg−1), Ammonium (mg N kg−1), Total amino acids (Aa) (μmol kg−1), Soil organic matter (SOM) (%), Microbial biomass C (MBC) (mg C kg−1), Microbial biomass N (MBN) (mg N kg−1).

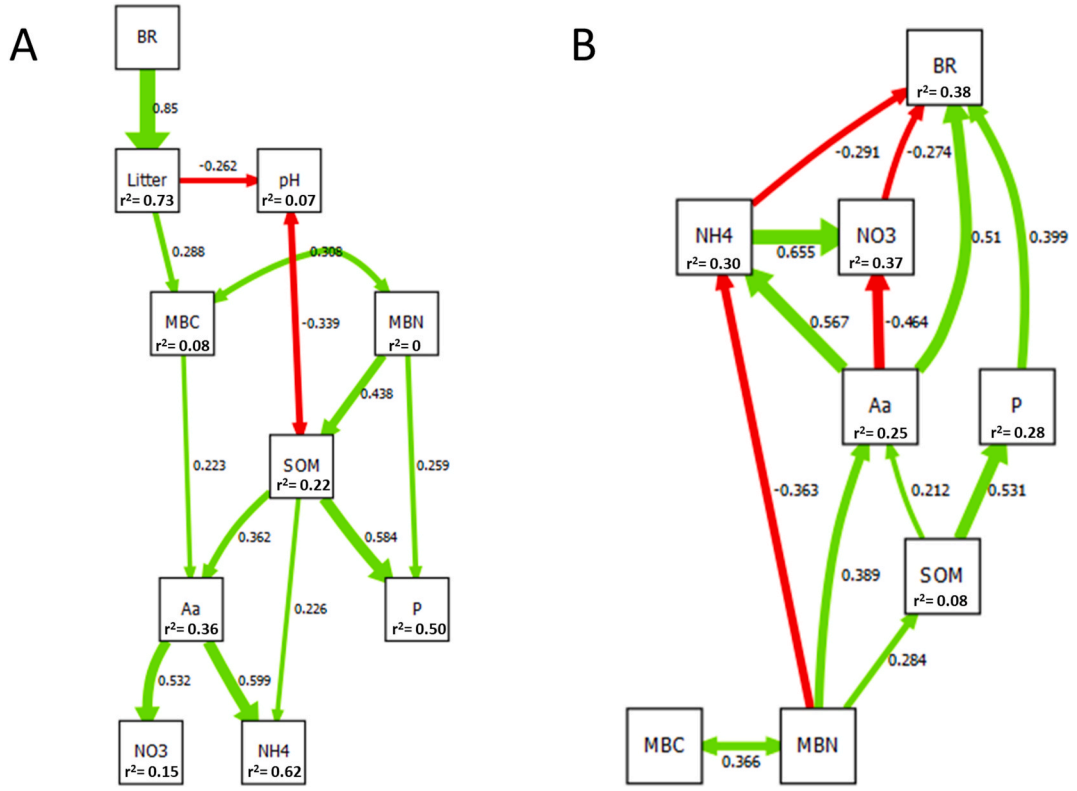

Fig. 6. Structural equation models for the model in the *B. rupestre*-patchy grassland (A) and the model in the *B. rupestre*-monodominant grassland (B). Boxes indicate measured variables. Arrows represent unidirectional relationships among variables. Green and red arrows indicate positive and negative relationships, respectively. Doubled-headed arrows represent correlations. Non-significant paths ($p \geq 0.05$) are not represented, except the pathway between MBN and SOM in B ($p = 0.052$). The thickness of each significant path is scaled according to the magnitude of the standardized regression coefficient displayed next to the arrow. r^2 values indicate percentages of variance explained. BR, *B. rupestre*; SOM, soil organic matter; Aa, amino acids; MBC, microbial biomass carbon; MBN, microbial biomass nitrogen. (For interpretation of the references to colour in this figure legend, the reader is referred to the Web version of this article.)

be partially explained by increases in microbial biomass and SOM. We found 'fertility islands' with higher concentrations of P and amino acids (but not other nutrients such as nitrate and ammonium) than in the surrounding areas under *B. rupestre* patches (Figs. 4 and 5). The spatial patterns of amino acids and P patches coincided with the spatial patterns of *B. rupestre* biomass, but not the ammonium patches Fig. 5), and we detected no significant spatial structure in nitrate availability at the scale of the study (Fig. 3 and Table 3). Hurst and John (1999) found that nitrate accumulated under *B. pinnatum* patches in chalk grasslands with soil pH over 7, but in our acidic soil the dominant form of mineral N is ammonium (Table 2) and the slow rates of nitrification expected at low pH may prevent nitrate accumulation.

The distribution of amino acid and P contents can be partially explained by SOM accumulation under *B. rupestre* patches. Litter inputs from *B. rupestre* were positively correlated with microbial biomass directly and with SOM indirectly, via a positive correlation with soil microbial biomass and a negative correlation with pH (Fig. 6a). Litter inputs can either increase or decrease soil pH, depending on the litter's ability to supply exchangeable base cations and initial pH of the soil (Sayer, 2006). In our poor-nutrient and acid soil, litter inputs from *B. rupestre* shoot biomass showed a negative correlation with soil pH, probably due to the inverse relationship between residence times of SOM fractions (coarse and labile) and soil pH, at least within a relevant pH range of 3.9–5.9 according to Leifeld et al. (2013).

However, the mismatches in spatial patterns of *B. rupestre* patches and both soil microbial biomass and SOM patches (Fig. 5), together with the low amount of variance explained by the SEM (r^2 for MBC = 0.08; MBN = 0, and SOM = 0.22) indicate that factors other than *B. rupestre* biomass and litter inputs are the main determinants of soil microbial biomass and SOM. Other factors that may contribute to microbial biomass growth and SOM accumulation (and ultimately soil fertility) include microclimate, litter quality and C inputs from belowground plant biomass. C inputs from rhizodeposition and root decomposition are retained longer in soils than those from aboveground tissues (Rasse et al., 2005), so their role in microbial growth and SOM accumulation could be even more important. However, in the *B. rupestre* patchy grassland we found no significant differences in amounts of total belowground biomass between *B. rupestre* patches and high diversity patches. We also detected no spatial structure in total belowground biomass in the top 10 cm of the patchy grassland. However, the C to N ratio of the belowground biomass probably differs between *B. rupestre* and diverse patches, since the proportion of legumes in the latter is greater.

4.2. Relationships between above- and below-ground spatial patterns in the monodominant grassland

In the frequently burned monodominant grassland, the lack of spatial structure in the vegetation cover (Tables 2 and 3) prevented analysis of the spatial associations between *B. rupestre* biomass and soil parameters. However, the homogeneous distribution of *B. rupestre* biomass was not reflected in homogeneous distributions of the soil variables. Most of the measured soil parameters had more heterogeneous spatial patterns in the monodominant grassland than in the patchy grassland: their coefficients of variation (Table 2) were similar or higher, whereas their autocorrelation ranges were similar or shorter, except for ammonium (Table 3).

The frequent burnings could maintain or even increase the spatial heterogeneity of soil properties in the monodominant grassland. Fire can alter soils' mineral nutrient contents and distributions through heating

(which enhances mineralization, pyrolysis and volatilization) and ash deposition (Rice, 1993). The post-fire distribution of microbial biomass may be driven by changes in microbial microhabitats and resource availability (Smithwick et al., 2012). Fire ashes' deposition and redistribution may be key determinants of spatial patterns of soil nutrients and microbial biomass. Our results suggest that spatial patterns of soil parameters in the monodominant grassland may be driven by the frequent fire regime.

Regarding organic matter, effects of fire on soil organic C depend on the temperature: significant consumption of organic matter starts at around 200 °C and it is completely consumed at around 460 °C (Giovannini et al., 1988). In the study area, the soil temperature reached in the burnings is unlikely to trigger significant losses of organic matter and nutrients through volatilization or pyrolysis except in the top millimetres of the soil (Múgica et al., 2018; San Emeterio et al., 2016). Frequently burned soils in the *B. rupestre* monodominant grassland had lower SOM contents than soils in the *B. rupestre* patchy grassland (Table 2). This was probably at least partly due to reductions in litter inputs caused by recurrent elimination of the vegetation by combustion, which causes marked declines in soil C stocks over time according to a recent meta-analysis (Xu et al., 2021).

Since we had no data on the spatial distribution *B. rupestre* biomass pre-burning, or spatial patterns of ash distribution, resource inputs into the soil in the monodominant grassland could not be modelled top-down. Instead, we applied a bottom-up approach to test effects of soil nutrients on *B. rupestre* shoot biomass. SEM revealed tendencies for P and amino acids to accumulate in the soil and immobilization of mineral N with strong competition between microbial populations and *B. rupestre* (Fig. 6b). According to this model, in contrast to the patchy grassland model, pH had no apparent effects on SOM or indirectly on nutrient availability, probably due to absence of the potential effect of litter addition.

4.3. Limitations of the study and future research

Although our hypothesis was partially accepted, the huge sampling effort needed for our spatially explicit approach and analysis of fresh samples required to characterize microbial processes did not allow appropriate replicate sampling to extrapolate the results beyond the plot- and time-scale (late spring period). However, many interesting patterns were detected in this complex study, which may inform future research that includes more replicates and considers, for instance, potential feedback effects of the amount and quality of the resource inputs (litter, ashes and belowground biomass) during the following growing seasons.

Declaration of competing interest

The authors declare that they have no known competing financial interests or personal relationships that could have appeared to influence the work reported in this paper.

Acknowledgements

The study was funded by "la Caixa" Foundation, Spain and CAN foundation, Spain (LCF/PR/PR13/51080004), the Ministry of Science and Innovation of the Spanish Government (project refs. CGL2010-21963, CGL2011-29746 and CGL2017-85490-R), and Interreg Sudoe Programme, European Regional Development Fund, European-Union, Open2preserve Project (SOE2/P5/E0804). L. Múgica and M. Durán were funded through a UPNA Research Staff Training Grant. The authors are grateful to the Livestock Board and forest rangers of the Aezkoa Valley for their support and to Asier Elkarte for his help during field work J.J. Jiménez acknowledges support from the ARAID Foundation, Spain.

Appendix A. Supplementary data

Supplementary data to this article can be found online at https://doi.org/10.1016/j.soilbio.2021.108455.

References

Bjornstad, O.N., 2018. ncf: spatial covariance functions. R package version 1.2-6.
Bollen, K.A., Pearl, J., 2013. Eight myths about causality and structural equation models. In: Morgan, S.L. (Ed.), Handbook of Causal Analysis for Social Research. Springer, pp. 301–328. https://doi.org/10.1007/978-94-007-6094-3_15.
Borcard, D., Gillet, F., Legendre, P., 2018. Spatial analysis of ecological data. In: Numerical Ecology with R. Springer International Publishing, Cham, pp. 299–367. https://doi.org/10.1007/978-3-319-71404-2_7.
Cambardella, C.A., Elliott, E.T., 1994. Carbon and nitrogen dynamics of soil organic matter fractions from cultivated grassland soils. Soil Science Society of America Journal 58, 123–130. https://doi.org/10.2136/sssaj1994.03615995005800010017x.
Canals, R.M., Múgica, L., Durán, M., Emeterio, L.S., 2019. Soil bacterial functional diversity mirrors the loss of plant diversity by the expansion of a native tall-grass in high mountain grasslands. Plant and Soil 445, 243–257. https://doi.org/10.1007/s11104-019-04281-w.
Canals, R.M., San Emeterio, L., Durán, M., Múgica, L., 2017. Plant-herbivory feedbacks and selective allocation of a toxic metal are behind the stability of degraded covers dominated by *Brachypodium pinnatum* in acidic soils. Plant and Soil 415, 373–386. https://doi.org/10.1007/s11104-016-3153-1.
Catorci, A., Cesaretti, S., Gatti, R., Ottaviani, G., 2011. Abiotic and biotic changes due to spread of *Brachypodium genuense* (DC.) Roem. & Schult. in sub-Mediterranean meadows. Community Ecology 12, 117–125. https://doi.org/10.1556/ComEc.12.2011.1.14.
Cressie, N.A.C., 1993. Statistics for Spatial Data. John Wiley & Sons, New York.
Darrouzet-Nardi, A., Ladd, M.P., Weintraub, M.N., 2013. Fluorescent microplate analysis of amino acids and other primary amines in soils. Soil Biology and Biochemistry 57, 78–82. https://doi.org/10.1016/j.soilbio.2012.07.017.
Das Gupta, S., MacKenzie, M.D., Quideau, S.A., 2015. Using spatial ecology to examine above and belowground interactions on a reclaimed aspen stand in northern Alberta. Geoderma 259–260, 12–22. https://doi.org/10.1016/j.geoderma.2015.04.004.
Davidson, E.A., Eckert, R.W., Hart, S.C., Firestone, M.K., 1989. Direct extraction of microbial biomass nitrogen from forest and grassland soils of California. Soil Biology and Biochemistry 21, 773–778.
German, D.P., Weintraub, M.N., Grandy, a.S., Lauber, C.L., Rinkes, Z.L., Allison, S.D., 2011. Optimization of hydrolytic and oxidative enzyme methods for ecosystem studies. Soil Biology and Biochemistry 43, 1387–1397. https://doi.org/10.1016/j.soilbio.2011.03.017.
Giovannini, G., Lucchesi, S., Giachetti, M., 1988. Effect of heating on some physical and chemical parameters related to soil aggregation and erodibility. Soil Science 146, 255–261.
Gobierno de Navarra. n.d. No Title [WWW Document]. http://meteo.navarra.es/climatologia/selfichaclima.cfm?IDEstacion=32&tipo=AUTO. accessed 6.3.20.
Gräler, B., Pebesma, E.J., Heuvelink, G., 2016. Spatio-temporal interpolation using gstat. The R Journal 8, 204–218.
Gutiérrez, J.R., Meserve, P.L., Contreas, L.C., Vásquez, H., Jaksic, F.M., 1993. Spatial distribution of soil nutrients and ephemeral plants underneath and outside the canopy of *Porlieria chilensis* shrubs (Zygophyllaceae) in arid coastal Chile. Oecologia 95, 347–352. https://doi.org/10.1007/BF00320987.
Holub, P., Tuma, I., Fiala, K., 2012. The effect of nitrogen addition on biomass production and competition in three expansive tall grasses. Environmental Pollution 170, 211–216.
Hurst, A., John, E., 1999. The biotic and abiotic changes associated with *Brachypodium pinnatum* dominance in chalk grassland in south-east England. Biological Conservation 88, 75–84. https://doi.org/10.1016/S0006-3207(98)00089-5.
Jiménez, J.-J., Decaëns, T., Amézquita, E., Rao, I., Thomas, R.J., Lavelle, P., 2011. Short-range spatial variability of soil physico-chemical variables related to earthworm clustering in a neotropical gallery forest. Soil Biology and Biochemistry 43, 1071–1080. https://doi.org/10.1016/j.soilbio.2011.01.028.
Jiménez, J.J., Decaëns, T., Lavelle, P., Rossi, J.-P., 2014. Dissecting the multi-scale spatial relationship of earthworm assemblages with soil environmental variability. BMC Ecology 14, 26. https://doi.org/10.1186/s12898-014-0026-4.
Joergensen, R.G., Wu, J., Brookes, P.C., 2011. Measuring soil microbial biomass using an automated procedure. Soil Biology and Biochemistry 43, 873–876. https://doi.org/10.1016/j.soilbio.2010.09.024.
Jones, D.L., Owen, A.G., Farrar, J.F., 2002. Simple method to enable the high resolution determination of total free amino acids in soil solutions and soil extracts. Soil Biology and Biochemistry 34, 1893–1902. https://doi.org/10.1016/S0038-0717(02)00203-1.
Kandeler, E., Gerber, H., 1988. Short-term assay of soil urease activity using colorimetric determination of ammonium. Biology and Fertility of Soils 6, 68–72. https://doi.org/10.1007/BF00257924.
Klironomos, J.N., 2002. Feedback with soil biota contributes to plant rarity and invasiveness in communities. Nature 417, 67–70. https://doi.org/10.1038/417067a.
Lefcheck, J.S., 2016. piecewiseSEM: piecewise structural equation modelling in r for ecology, evolution, and systematics. Methods in Ecology and Evolution 7, 573–579. https://doi.org/10.1111/2041-210X.12512.

Legendre, P., Fortin, M.J., 1989. Spatial pattern and ecological analysis. Vegetatio 80, 107–138. https://doi.org/10.1007/BF00048036.
Leifeld, J., Bassin, S., Conen, F., Hajdas, I., Egli, M., Rg Fuhrer, J., 2013. Control of soil pH on turnover of belowground organic matter in subalpine grassland. Biogeochemistry 112, 59–69. https://doi.org/10.1007/s10533-011-9689-5.
Múgica, L., Canals, R.M., San Emeterio, L., 2018. Changes in soil nitrogen dynamics caused by prescribed fires in dense gorse lands in SW Pyrenees. The Science of the Total Environment 639, 175–185. https://doi.org/10.1016/j.scitotenv.2018.05.139.
Pinheiro, J., Bates, D., DebRoy, S., Sarkar, D., the R Core Team, 2018. nlme: Linear and Nonlinear Mixed Effects Models.
R Core Team, 2018. R: A Language and Environment for Statistical Computing.
Rasse, D.P., Rumpel, C., Dignac, M.F., 2005. Is soil carbon mostly root carbon? Mechanisms for a specific stabilisation. Plant and Soil 269, 341–356. https://doi.org/10.1007/s11104-004-0907-y.
Rice, S.K., 1993. Vegetation establishment in post-fire *Adenostoma* chaparral in relation to fine-scale pattern in fire intensity and soil nutrients. Journal of Vegetation Science 4, 115–124. https://doi.org/10.2307/3235739.
Rietkerk, M., van de Koppel, J., 1997. Alternate stable states and threshold effects in semi-arid grazing systems. Oikos 79, 69–76. https://doi.org/10.2307/3546091.
Rodríguez-Loinaz, G., Onaindia, M., Amezaga, I., Mijangos, I., Garbisu, C., 2008. Relationship between vegetation diversity and soil functional diversity in native mixed-oak forests. Soil Biology and Biochemistry 40, 49–60. https://doi.org/10.1016/j.soilbio.2007.04.015.
San Emeterio, L., Canals, R.M., Herman, D.J., 2014. Combined effects of labile and recalcitrant carbon on short-term availability of nitrogen in intensified arable soil. European Journal of Soil Science 65, 377–385. https://doi.org/10.1111/ejss.12133.
San Emeterio, L., Múgica, L., Ugarte, M.D., Goicoa, T., Canals, R.M., 2016. Sustainability of traditional pastoral fires in highlands under global change: effects on soil function and nutrient cycling. Agriculture, Ecosystems & Environment 235, 155–163. https://doi.org/10.1016/j.agee.2016.10.009.
Sayer, E.J., 2006. Using experimental manipulation to assess the roles of leaf litter in the functioning of forest ecosystems. Biological Reviews of the Cambridge Philosophical Society. https://doi.org/10.1017/S1464793105006846.
Schlesinger, W.H., Pilmanis, A.M., 1998. Plant-soil interactions in deserts. Biogeochemistry 42, 169–187. https://doi.org/10.1023/A:1005939924434.
Smithwick, E.A.H., Naithani, K.J., Balser, T.C., Romme, W.H., Turner, M.G., 2012. Post-fire spatial patterns of soil nitrogen mineralization and microbial abundance. PLoS One 7, e50597. https://doi.org/10.1371/journal.pone.0050597.
Suding, K.N., Gross, K.L., Houseman, G.R., 2004. Alternative states and positive feedbacks in restoration ecology. Trends in Ecology & Evolution 19, 46–53. https://doi.org/10.1016/j.tree.2003.10.005.
Suding, K.N., Stanley Harpole, W., Fukami, T., Kulmatiski, A., MacDougall, A.S., Stein, C., van der Putten, W.H., 2013. Consequences of plant-soil feedbacks in invasion. Journal of Ecology 101, 298–308. https://doi.org/10.1111/1365-2745.12057.
Úbeda, X., Lorca, M., Outeiro, L.R., Bernia, S., Castellnou, M., Ubeda, X., Lorca, M., Outeiro, L.R., Bernia, S., Castellnou, M., 2005. Effects of prescribed fire on soil quality in Mediterranean grassland (Prades Mountains, north-east Spain). International Journal of Wildland Fire 14, 379–384. https://doi.org/10.1071/WF05040.
van der Putten, W.H., Bardgett, R.D., Bever, J.D., Bezemer, T.M., Casper, B.B., Fukami, T., Kardol, P., Klironomos, J.N., Kulmatiski, A., Schweitzer, J.A., Suding, K.N., de Voorde, T.F.J., Wardle, D.A., 2013. Plant-soil feedbacks: the past, the present and future challenges. Journal of Ecology 101, 265–276. https://doi.org/10.1111/1365-2745.12054.
Vinton, M.A., Goergen, E.M., 2006. Plant-soil feedbacks contribute to the persistence of *Bromus inermis* in tallgrass prairie. Ecosystems 9, 967–976. https://doi.org/10.1007/s10021-005-0107-5.
Xu, S., Sayer, E.J., Eisenhauer, N., Lu, X., Wang, J., Liu, C., 2021. Aboveground litter inputs determine carbon storage across soil profiles: a meta-analysis. Plant and Soil 1–16. https://doi.org/10.1007/s11104-021-04881-5.